Contents lists available at ScienceDirect

Solid State Communications

Vibrational modes in the Pmc2$_1$ structure of ZnGeN$_2$

Mark Hagemann, Churna Bhandari, Walter R.L. Lambrecht *

Department of Physics, Case Western Reserve University, 10900 Euclid Avenue, Cleveland, OH 44106-7079, USA

ARTICLE INFO

ABSTRACT

Vibrational normal modes at the Brillouin zone center and related Raman and infrared spectra are calculated from first-principles density functional perturbation theory for the until now hypothetical Pmc2$_1$ structure of ZnGeN$_2$ and are compared with those in the known Pnb2$_1$ structure. Although there are great similarities in phonon spectra, we show that the distinctions are specific enough to experimentally distinguish the two crystal structures.

1. Introduction

ZnGeN$_2$ is a heterovalent ternary semiconductor closely related to GaN. It is derived from it conceptually by replacing the four nearest neighbor Ga around each N in the wurtzite structure by two Zn and two Ge atoms. This ensures the local charge neutrality since each Zn is divalent, each Ge is four-valent and Ga is three valent. While the known crystal structure of ZnGeN$_2$ and other II–IV-Nitrides has a 16 atom cell with space group Pna2$_1$, [1,2] it was recently suggested that another crystal structure with spacegroup Pmc2$_1$ could have very close energy to this structure [3]. More precisely this structure was suggested for ZnSnN$_2$ and in that work found to have the same energy as Pna2$_1$ within the precision of the calculations.

Subsequently, it was shown by Quayle et al. [4] that disordered forms of both ZnGeN$_2$ and ZnSnN$_2$ could be viewed as a mixture at the atomic scale of these two crystal structures. They both contain rows of atoms in the basal plane which have alternating Zn and Ge atoms but are simply stacked slightly differently. As a result, a one dimensional type of disorder can result by randomly changing the stacking. It is important to note that both structures obey the octet rule locally. That is, each tetrahedron has two Zn and two Ge instead of for instance one Zn and three Ge or vice versa. Structures which contain such octetrule violating local environments were found to have significantly higher energy.

The two crystal structures are shown in Fig. 1. The difference in structure between Pmc2$_1$ and Pna2$_1$ shown in Fig. 1 is rather subtle. First note that with our chosen setting of the axes, we should really label the space group Pnb2$_1$. The Pmc2$_1$ structure has an ordinary mirror plane (labeled m corresponding to the $bc=yz$ plane in our choice of axes) instead of a glide mirror plane (labeled

b corresponding to translation $\mathbf{b}/2$ in the plane) and one glide mirror-plane c with translation in only one crystallographic direction (lying in the $ac=xz$ plane with translation $\mathbf{c}/2$) instead of a diagonal glide mirror-plane (n with translation $(\mathbf{a}+\mathbf{c})/2$). Both spacegroups have twofold screw axes but in Pmc2$_1$ they are located at the intersection of the mirror planes, while in Pnb2$_1$ they lie halfway in between them. The unit cell has only 8 atoms. The two structures correspond simply to a $1 \times \sqrt{3}$ and $2 \times \sqrt{3}$ superlattice of the wurtzite lattice along the so-called ortho-hexagonal axes. Both structures are orthorhombic. In Quale et al. [4] it was shown that for ZnGeN$_2$ the energy difference between the two structures is slightly larger than for ZnSnN$_2$. Although thus far only the Pnb2$_1$ structure has been observed as ordered arrangement of the cations in ZnGeN$_2$ or any other II–IV-nitride we know of, a disordered phase has been found for ZnGeN$_2$ as well and in ZnSnN$_2$ only the disordered phase has been observed. At present it is not at all clear how one would stabilize the Pmc2$_1$ structure or if it could occur as a "growth accident" in small regions within disordered ZnGeN$_2$. Nonetheless, it is of some interest to predict how its properties would differ. In particular, the vibrational modes could provide a sensitive way to identify the structure via for example Raman spectroscopy or infrared absorption spectroscopy. Thus in this paper we study how the vibrational normal modes and the associated Raman and infrared spectra differ between the two structures.

2. Computational methods

The calculations were performed within density functional perturbation theory [5,6] using a plane wave basis set and norm-conserving pseudopotentials of the Fritz–Haber type. [7] The calculations were performed using the ABINIT code [8]. In addition,

* Corresponding author.

we also tested Hartwigsen, Goedecker, Hutter (HGH) pseudopotential [9]. The plane wave energy cut-off was chosen similar to that in previous work [10], higher than 80 Hartree. The structures were relaxed until the residual forces were smaller than 10^{-5} Hartree/Bohr. The exchange correlation potential was modeled in the local density approximation (LDA) [11]. Brillouin zone integrations in the electronic structure portion of the calculations were carried out with a $8 \times 4 \times 4$ Monkhorst–Pack mesh for the $Pmc2_1$ and $4 \times 4 \times 4$ for the $Pnb2_1$ structure, respectively. These are chosen to be equivalent in terms of reciprocal space sampling because $Pmc2_1$ has half the a lattice constant size of $Pnb2_1$ and thus twice as large a Brillouin zone size in this direction. Calculations with a smaller $2 \times 2 \times 2$ mesh for $Pnb2_1$ agreed on the phonons to be better than 1%. For phonon band structure and density of states calculations, which rely on interpolation from a separate mesh for the phonons, we used a $4 \times 2 \times 2$ Monkhorst–Pack mesh for $Pmc2_1$ and $2 \times 2 \times 2$ for $Pnb2_1$ structure. The energy cut-off was slightly reduced to 70 Hartree for the phonon calculations to speed up the calculation without loss of accuracy.

3. Results

Group theory is used to analyze the number of vibrational modes of each type. The point group for both structures is C_{2v} and contains four irreducible representations. Among these a_1, b_1, and b_2 are infrared active for polarizations along z, x, and y. The latter are chosen along the c, a, and b directions of the crystal, respectively.

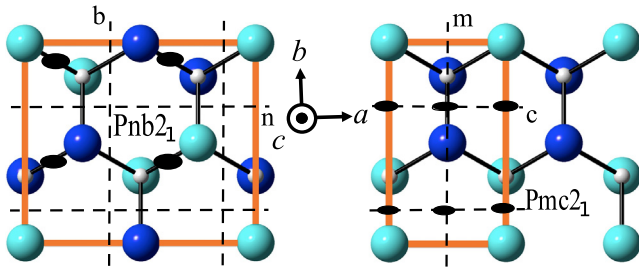The character table can be found for example in Ref. [12]. The a_2 mode is even under rotation about the z-axis but odd under both mirror planes. All modes are Raman active and the polarizations for which there are non-zero Raman tensor components are also indicated in Table 1.

Table 1 also lists the number of modes of each type in both crystal structures. Thus clearly, already from the different number of modes one should, in principle, be able to distinguish the two crystal structures. The mode frequencies for the $Pmc2_1$ and $Pnb2_1$ are given in Table 1. Although the ones for $Pnb2_1$ have been reported before in Refs. [13,10], we here repeated the calculations for both structures, to make sure all computational parameters such as choice of exchange correlations and various convergence parameters are identical for both. Good agreement is obtained with Paudel et al. [10] for $Pnb2_1$. When using the HGH pseudopotential, the relaxed lattice constants agreed with the FHI pseudopotential to be better than 1%. The phonons showed at most a 2% change.

In Figs. 2 and 3, we show the infrared spectra for $Pmc2_1$ and $Pnb2_1$, respectively. For each mode, we show the real and imaginary parts of the dielectric function, the loss function $-\mathrm{Im}\{\varepsilon(\omega)^{-1}\}$ and the reflectivity. The imaginary part of the dielectric function has peaks at the TO modes, the real part has zeros at the LO modes and the loss function has peaks at the LO modes. The reflectivity shows the well-known Reststrahlen bands. We can see that in spite of the different number of modes, the a_1 spectra look
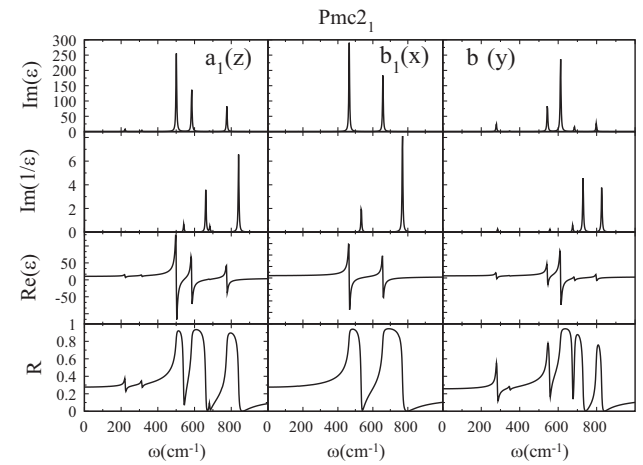

Fig. 1. (Color online) Crystal structures of $Pnb2_1$ (left) and $Pmc2_1$ (right).

Fig. 2. IR spectrum in $Pmc2_1$ crystal structure.

Table 1
Phonons frequency of $ZnGeN_2$ for 8 atom cell $Pmc2_1$ and 16 atom cell $Pnb2_1$ in unit of cm^{-1}.

Freq.	$Pmc2_1$	$Pnb2_1$	Mode	Basis
$n(a_1)$	7	11	a_1(IR/Raman)	z,x^2,y^2,z^2
ω_{TO}	137, 222, 312, 501, 585, 681, 775	135, 170, 192, 224, 300, 482, 485, 587, 623, 758, 765		
ω_{LO}	137, 224, 313, 541, 662, 684, 840	135, 170, 192, 226, 301, 482, 527, 623, 668, 765, 827		
$n(a_2)$	4	12	a_2(Raman)	xy
ω	124, 141, 456, 644	132, 163, 184, 201, 267, 341, 471, 554, 579, 655, 753, 818		
$n(b_1)$	3	11	b_1(IR/Raman)	x,xz
ω_{TO}	174, 465, 658	168, 194, 239, 308, 325, 511, 550, 597, 652, 769, 813		
ω_{LO}	174, 501, 777	169, 194, 240, 310, 325, 537, 557, 651, 708, 796, 824		
$n(b_2)$	7	11	b_2(IR/Raman)	y,yz
ω_{TO}	173, 278, 347, 544, 613, 685, 798	130, 167, 209, 267, 339, 480, 506, 601, 671, 776. 791		
ω_{LO}	173, 285, 348, 557, 676, 732, 828	130, 167, 211, 267, 339, 490, 561, 630, 671, 790, 863		